Energy & Environmental Science

Accepted Manuscript

ROYAL SOCIETY OF CHEMISTRY

www.rsc.org/ees

Cite this: DOI: 10.1039/c0xx00000x

www.rsc.org/xxxxxx

ARTICLE TYPE

Quasi Core-Shell Nitrogen-Doped Graphene/Cobalt Sulfide Conductive Catalyst for Highly Efficient Dye-Sensitized Solar Cells**

Enbing Bi, [a] Han Chen,*[a] Xudong Yang,[b] Wenqin Peng,[b] Michael Grätzel[c] and Liyuan Han*[a, b]

Received (in XXX, XXX) Xth XXXXXXXXX 20XX, Accepted Xth XXXXXXXXX 20XX

DOI: 10.1039/b000000x

A novel conductive catalyst was designed based on a quasi core/shell structure of N-doped graphene/cobalt sulfide. This Platinum-free catalyst shows high catalytic activity and conductivity owing to close interactions between the core-cobalt sulphide and the shell- N-doped graphene. It enables dye-sensitized solar cells (DSSCs) to obtain high energy conversion efficiency up to 10.71%, which is as far as we know the highest efficiency for DSSCs based on Platinum-free counter electrode.

Dye-sensitized solar cells (DSSCs) are promising photovoltaic devices, primarily because of their low cost and high efficiency.[1–4] A standard DSSC has three main components: a dye-sensitized TiO_2 photoanode, an iodide/triiodide (I^-/I_3^-) redox electrolyte, and a counter electrode (CE). The CE plays a key role in improving device performance by catalyzing reduction of the electrolyte, which mediates regeneration of the sensitizer after electron injection. The conventional material for CEs is Pt, which has remarkably high conductivity and efficiently catalyzes the reduction of I_3^- to I^-. However, large-scale commercial application of Pt-containing DSSCs is seriously hindered by the high cost and low abundance of Pt.[5] Hence, much effort has been devoted to the development of alternative CE materials, such as carbon materials,[6,7] conductive polymer materials,[8,9] and inorganic materials.[10–12]

The ideal CE material should, like Pt, have not only excellent catalytic activity but also high conductivity.[13,14] However, obtaining a single material with both properties has proved to be difficult. For example, carbon materials show poor catalytic performance, and conductive polymers are not sufficiently stable. In addition, CEs containing various inorganic materials, such as transition-metal sulfides,[15] selenides,[16] carbides,[17] and nitrides,[18] show excellent catalytic activity and good thermal stability, but their conductivity is low, owing to abundant grain boundaries and defects.[19] Recently, hybrid materials, such as TiN/carbon nanotubes,[20] CoS/multiwall carbon nanotubes,[21] and NiS_2/reduced graphene oxide,[22] have been reported to show improved catalytic activity and conductivity relative to single-component materials, and use of these hybrid materials in DSSCs results in enhanced efficiency. However, the efficiency of cells fabricated with these hybrids is still lower than that of cells with Pt CEs, especially, in the cell with high efficiency of over 10%, this may because it lacks of a useful structure to generate a synergistic effect in the hybrid materials.

Here, inspired by the core-shell structure hybrid materials can provide superior electrochemical performance due to the positive synergistic effect,[23–26] we describe a novel quasi core–shell hybrid material that exhibits both high conductivity and excellent catalytic activity. The material consists of a core of CoS nanoparticles coated with a shell of ultrathin N-doped graphene (NDG) layers that act as conductive paths to overcome the problem of low conductivity due to grain boundaries and defects between the CoS nanoparticles. A DSSC prepared with this quasi core–shell NDG/CoS catalyst as the CE showed a high short-circuit current density (20.38 mA cm^{-2}) and an energy-conversion efficiency of 10.71%, which is, as far as we know, the highest reported efficiency for a DSSC based on a Pt-free CE.

The quasi core-shell NDG/CoS catalyst was synthesized from liquid-phase reactants by means of in-situ solvothermal self assembly method (see Supporting Information). The morphology of the as-prepared catalyst was examined by scanning electron microscopy and transmission electron microscopy. The scanning electron microscopy images showed an NDG/CoS sand film with homogeneously distributed CoS nanoparticles wrapped by several layers of silk-like NDG (Figure 1a, b). The NDG film can tightly attached to CoS nanoparticle surfaces. Energy-dispersive X-ray element mapping confirmed that C, N, Co, and S were uniformly distributed in the film (Figure 1c). The transmission electron microscopy images (Figure 1d–g) further confirmed the quasi core-shell structure and clearly demonstrated that the CoS nanoparticles had an average size of 20–50 nm. The CoS nanoparticles had relatively high crystallinity and were encapsulated by an ultrathin (2 ± 0.3 nm) NDG shell with the traditional (001) plane; the lattice constants of CoS were 0.254 and 0.193 nm, corresponding to the (101) and (102) planes, respectively. [27] Moreover, the transmission electron microscopy images showed that the NDG shell was seamlessly wrapped around the CoS nanoparticles, indicating a strong interaction between the core and the shell. For comparison, we also synthesized the N-undoped graphene/CoS (G/CoS) under the same conditions in the absence of ammonia, which is the N source for NDG/CoS. Under these conditions, the CoS nanoparticles were uniformly distributed on the reduced graphene oxide, but they were not encapsulated by the graphene to form a core–shell structure (Supporting Information, Figure S1a–c). This result indicates that ammonia facilitated formation of the quasi

core–shell structure of NDG/CoS, probably because ammonia changed the pH values of solution and resulted in the aggregation of graphene nanosheets on the CoS particles.

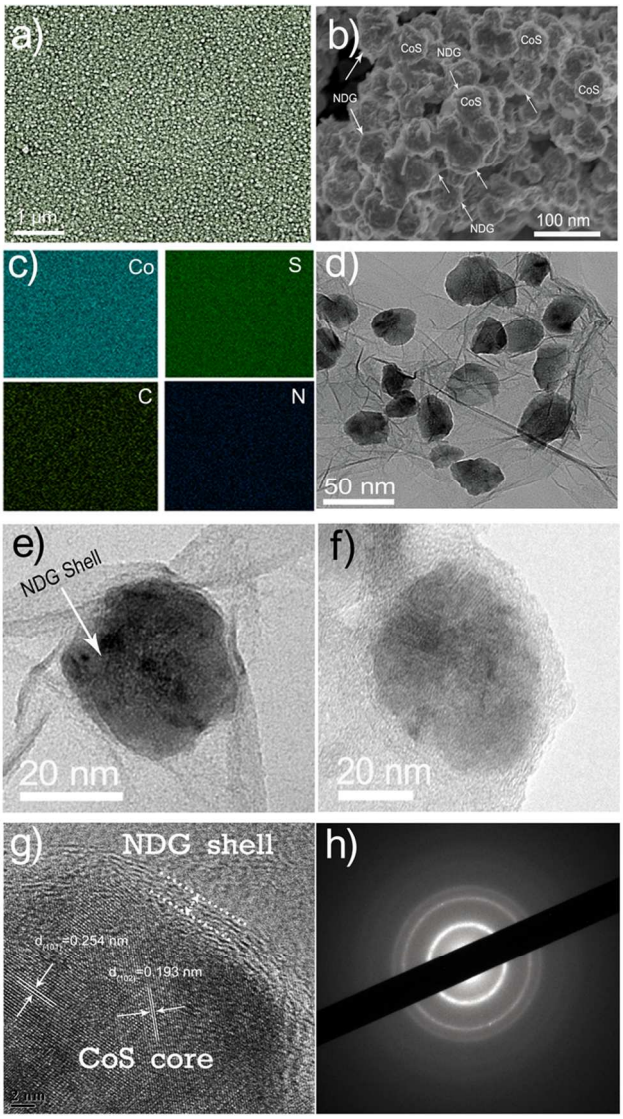

Figure 1.a, b) Scanning electron microscopy images and c) element distribution mapping images of an NDG/CoS film on a fluorine-doped tin oxide glass substrate (the white arrow refers to the NDG shell); d, e, f) Transmission electron microscopy images of NDG/CoS; g) High-resolution transmission electron microscopy image of NDG/CoS. h) Selected-area electron diffraction pattern of NDG/CoS.

The diffraction rings of the selected-area electron diffraction pattern (Figure 1h) corresponded to the crystalline planes of the NDG/CoS. This result was confirmed by X-ray powder diffraction (Figure S2). The (100), (101), (102), and (110) planes in the NDG/CoS could be readily indexed to the CoS. In addition, no apparent graphene peak could be identified at 20–30°, probably because of the low mass of NDG in the NDG/CoS in agreement with previously reported results for graphene-based materials[27] or because the ultrathin NDG homogeneously distributed on the surface of the CoS nanoparticles formed a closed interaction with the nanoparticles, in agreement with the transmission electron microscopy results (Figure 1).[28, 29] Moreover, the X-ray diffraction pattern of G/CoS revealed the presence of $CoS_{1.097}$ and CoS_2 phases in addition to the CoS phase, which indicates that ammonia-assisted N doping facilitated formation of the pure CoS phase observed in the NDG/CoS.

To further investigate the bonding configurations of N and the changes caused by the N-doping process, we measured X-ray photoelectron spectra (Figure 2a), which confirmed the presence of Co, S, N, C, and O. The percentage of N in NDG/CoS was 5.8%, compared to 2.4% for NDG. The high-resolution N1s spectra of NDG/CoS and NDG (Figure 2b–c) revealed three N peaks, as described in previous reports.[30, 31] The two peaks at lower binding energies (about 398.8 and 400.6 eV) corresponded to pyridinic and pyrrolic N, respectively, which contribute electron density to the π-conjugated system with a pair of p-electrons in the graphene layer. The peak at 401.8 eV was due to N substituted for C within the graphene network, referred to as graphitic N. Among the total N state, NDG/CoS contained higher percentages of pyridinic N and graphitic N (15.01% and 58.52%, respectively; Figure 2d) than that in NDG. The increasing pyridinic N and graphitic N were more effective than the pyrrolic N at improving the electrochemical performance of NDG.[32] The positive effect of pyridinic and graphitic N has also been observed on oxygen reduction reaction.[33]Hence, we expect the quasi core-shell NDG/CoS will obtain higher catalyst activity due to the positive synergistic effect between NDG and CoS.

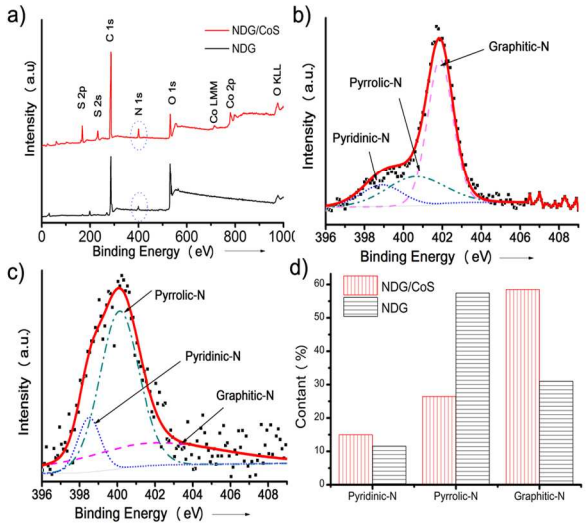

Figure 2.a) XPS survey spectra of NDG/CoS, G/CoS, NDG and graphene, high-resolution XPS N1s survey spectra of b) NDG/CoS, c) NDG, d) the percentage of three N1s peaks in NDG/CoS and NDG.

Additionally, the chemical reduction of grapheme can be positive to improve the conductivity of the graphene-based catalyst. [34, 35] The oxygen in the graphene was mainly in forms combined with C, such as C–O, C=O, and C=OO groups. Compared to grapheme oxide (GO), the oxygen species of C–O, C=O and O=C–O of the NDG, G/CoS and NDG/CoS reduced significantly and the major remaining species were C=C and C–C, indicating an efficient deoxidization by N-doping process and

thiourea reduction process (Figure S3b–f). Moreover, the oxygen content of NDG/CoS was lower than that of G/CoS and NDG (Figures 2a and S3a), due to the NDG/CoS contained substantially lower amounts of C=O and O=C–O with respect to G/CoS and NDG, may caused by triethanolamine's reduction of graphene.

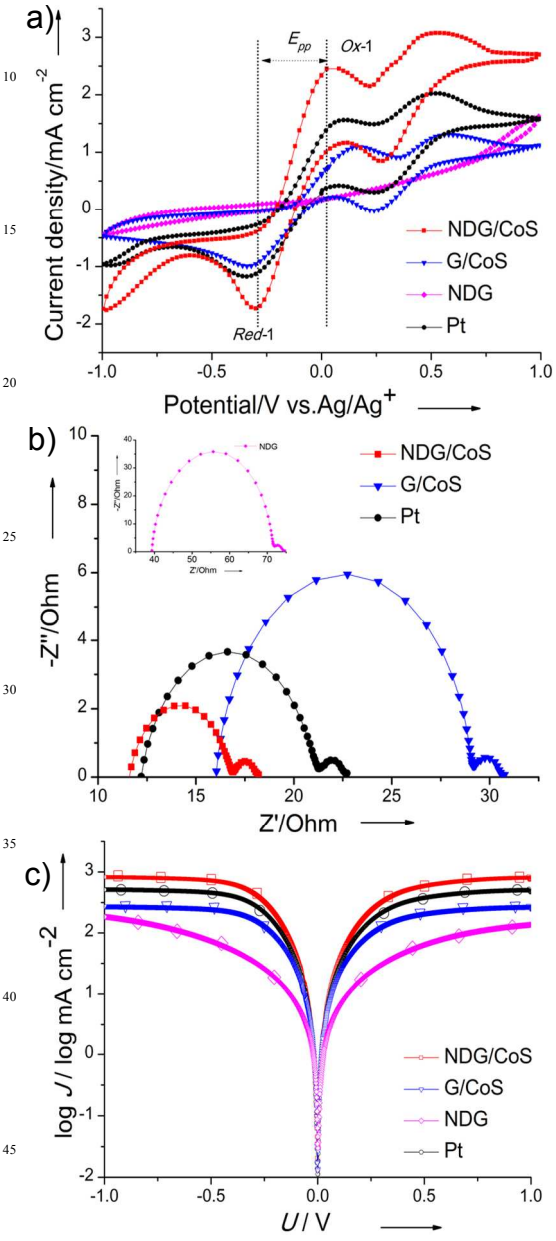

Figure 3. a) Cyclic voltammograms of NDG/CoS, G/CoS, NDG and Pt on a FTO glass substrate cycled in the I^-/I_3^- electrolyte (10 mM LiI, 1mM I_2, and 0.1M $LiClO_4$ in acetonitrile solution) at a scan rate of 50 mVs^{-1}, a Pt wire was used as the CE, and Ag/Ag^+ was used as the reference electrode. b) Nyquist plots of dummy cells with a symmetric sandwich-like structure fabricated with the four materials. The frequency scan ranged from 0.1 Hz to 1 MHz. c) Tafel polarization curves for the symmetrical cells fabricated in the same way as the ones used in the EIS experiments.

To evaluate the catalytic activity and conductivity of the quasi core–shell NDG/CoS, we performed cyclic voltammetry (CV) measurements and electrochemical impedance spectroscopy (EIS) and obtained Tafel polarization curves for a NDG/CoS electrode, as well as for G/CoS, NDG, and Pt electrodes for comparison. CV measurements were carried out with a three-electrode system and recorded between –1 V and 1 V (see the Supporting Information). Two typical pairs of oxidation and reduction peaks in the CV curves were clearly observed for all the electrodes except the NDG electrode (Figure 3). The left pair was attributed to the process shown in Eq. 1, and the right pair to the process shown in Eq. 2. Because the main function of the CE of a DSSC is to catalyze the reduction of I_3^- to I^-, which corresponds to the left pair of peaks (Ox-1 and Red-1) in the CV curves, the characteristics of these peaks were the main focus of our analysis. [36]

$$I_3^- + 2e^- \leftrightarrow 3I^- \quad (1)$$

$$3I_2 + 2e^- \leftrightarrow 2I_3^- \quad (2)$$

Generally, catalytic activity increases with increasing reduction peak current density and with decreasing peak-to-peak voltage separation (E_{pp}). The quasi core–shell NDG/CoS had a peak current density of 2.47 mA cm^{-2}, which was higher than the values for G/CoS and Pt. In addition, its E_{pp} of 310 mV (Table 1) was lower than the values for G/CoS and Pt. The fact that the quasi core–shell NDG/CoS electrode had a higher peak current density and lower E_{pp} than the other electrodes confirmed that it is a remarkably conductive catalyst for lowering the overpotential in the reduction of I_3^- to I^-, which favors regeneration of the sensitizer.[37]

Electrochemical impedance spectra were measured in cells consisting of a symmetric sandwich structure (electrode/electrolyte/electrode) with NDG/CoS, G/CoS, NDG, and Pt as electrodes (Figure 3b). The left semicircle was attributed to charge-transfer resistance (R_{ct}), which reflects the electrode's catalytic activity for I_3^- reduction; whereas the right semicircle was assigned to ionic diffusion impedance. Series resistance (R_s) can be obtained from the high-frequency intercept on the real axis. [38] The fit data for R_s and R_{ct} are listed in Table 1. Among the four electrodes, the NDG/CoS electrode exhibited the smallest R_{ct} (2.58 Ω), which indicates that it had excellent catalytic activity for reduction of I_3^- to I^- at the electrolyte/electrode interface; in fact, it was superior to Pt. Moreover, the R_s of NDG/CoS was a little lower than that of Pt and much lower than the values for G/CoS and NDG, which suggests that the NDG/CoS had excellent conductivity. The combination of lower R_{ct} and R_s leads to a decrease in the total internal resistance and thus to a high DSSC fill factor (FF).

To further demonstrate the charge-transfer properties of the I^-/I_3^- couple on the electrode surface, we conducted Tafel polarization measurements on the same cells used for EIS measurements (Figure 3c). [39] The slopes of the Tafel polarization curves decreased in the order NDG/CoS > Pt > G/CoS > NDG, which is consistent with the order of exchange current density. These results are in good agreement with the CV and EIS results.

Finally, we optimized the thickness of the quasi core–shell NDG/CoS as CEs for DSSCs (the Supporting Information, Figure

S4). The photoanode of the DSSCs was composed of an N749 dye-sensitized TiO_2 film on a fluorine-doped tin oxide glass plate, and I^-/I_3^- was used as the redox shuttle. Figure 4 shows the current density–voltage (*J–V*) curves of DSSCs with different CEs under irradiation at 100 mW cm^{-2} through a black metal mask with an aperture area of 0.25 cm^2,[40] and the photovoltaic parameters are summarized in the Table 1. The cell with the quasi core–shell NDG/CoS CE showed a short-circuit current density (J_{sc}) of 20.38 mA cm^{-2}, an open-circuit potential (V_{oc}) of 710 mV, a high FF of 0.74, and an energy-conversion efficiency (η) of 10.71%, which is a notable improvement compared to the efficiency observed with a Pt CE (9.73%) and a good repeatability (the Supporting Information, Figure S5). The cell with the NDG/CoS CE exhibited a much higher J_{sc} than the cells with G/CoS and NDG CEs because of the excellent activity of the doped quasi core–shell catalyst, and the J_{sc} value of the former was also slightly higher than that of the cell with a Pt CE. The J_{sc} results agreed well with the R_{ct} results obtained by means of EIS. In addition, the FF of the cell based on NDG/CoS was also higher than that of the Pt-based cell because the former had a low resistance for I_3^- reduction on the surface of the CE. The good photovoltaic characteristics of the quasi core–shell NDG/CoS CE confirmed that the hybrid material is a good conductive catalyst.

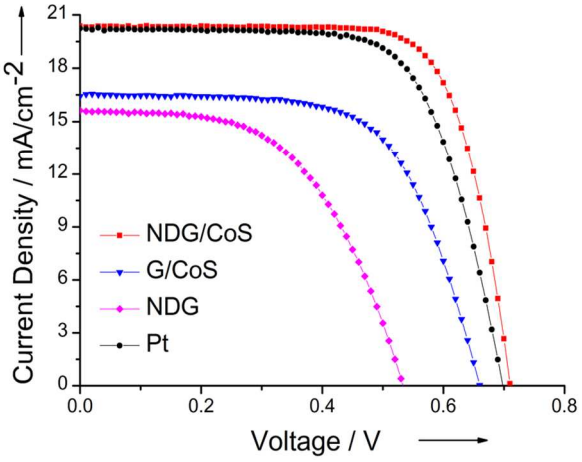

Figure 4. *J–V* characteristics of DSSCs with NDG/CoS, G/CoS, NDG, and Pt as counter electrodes measured under AM 1.5 illumination with a metal mask. The active area of DSSCs is 0.25 cm^{-2}.

Table 1: The detailed photovoltaic performance of the DSSCs using different CEs and the resulting data from CV and EIS spectra[a]

Devices	J_{sc} mA cm^{-2}	V_{oc} mV	FF	η %	R_s Ω	R_{ct} Ω	E_{pp} mV
NDG/CoS	20.38	710	0.74	10.71	11.58	2.58	0.31
G/CoS	16.42	660	0.65	7.05	16.06	6.57	0.50
NDG	15.53	534	0.54	4.49	39.34	16.21	——
Pt	20.21	698	0.69	9.73	12.23	4.62	0.40

[a] R_{ct}: charge-transfer resistance, R_S: series resistance were obtained from EIS; E_{pp}: peak-to-peak voltage separation was caculated from CV.

In summary, we synthesized a novel quasi core–shell NDG/CoS conductive catalyst. This hybrid material featured close interactions between the CoS core and the NDG shell, which imparted both high catalytic activity and high conductivity to the material. A DSSC fabricated with an NDG/CoS CE showed high energy-conversion efficiency, up to 10.71%, which is, as far as we know, the highest reported efficiency for a DSSC based on a Pt-free CE. The simple, low-cost assembly protocol will provide a new pathway for the large-scale production of various quasi core–shell NDG-based hybrid materials for application in energy-storage devices or optoelectronic devices.

Received: ((will be filled in by the editorial staff))
Published online on ((will be filled in by the editorial staff))

Notes and references

[a] *State Key Laboratory of Metallic Matrix Composites Materials, School of Materials Science and Engineering, Shanghai Jiao Tong University, Shanghai 200240, China. E-mail: chen.han@sjtu.edu.cn. Fax: (+86) 21-54742414, Tel: (+86) 21-54742414*
[b] *Photovoltaic Materials Unit, National Institute for Materials Science, Tsukuba, Ibaraki 305-0047 (Japan). HAN.Liyuan@nims.go.jp. Fax: (+81) 29-859-2304*
[c] *Laboratory of Photonics and Interfaces, Institute of Chemical Sciences and Engineering, École polytechnique fédérale de Lausanne, 1015 Lausanne (Switzerland)*

† Electronic Supplementary Information (ESI) available: [Quasi Core-Shell Nitrogen-Doped Graphene/Cobalt Sulfide Conductive Catalyst and fabrication of DSCs and symmetrical cells and characterization]. See DOI: 10.1039/b000000x/

1. B. O'regan and M. Grätzel, nature, 1991, 353, 737-740.
2. A. Yella, H.-W. Lee, H. N. Tsao, C. Yi, A. K. Chandiran, M. K. Nazeeruddin, E. W.-G. Diau, C.-Y. Yeh, S. M. Zakeeruddin and M. Grätzel, Science, 2011, 334, 629-634.
3. M. Wang, N. Chamberland, L. Breau, J.-E. Moser, R. Humphry-Baker, B. Marsan, S. M. Zakeeruddin and M. Grätzel, Nature chemistry, 2010, 2, 385-389.
4. Y. Chiba, A. Islam, Y. Watanabe, R. Komiya, N. Koide and L. Han, Japanese Journal of Applied Physics, 2006, 45, L638.
5. H. Wang, G. Liu, X. Li, P. Xiang, Z. Ku, Y. Rong, M. Xu, L. Liu, M. Hu and Y. Yang, Energy & Environmental Science, 2011, 4, 2025-2029.
6. M. Wu, X. Lin, T. Wang, J. Qiu and T. Ma, Energy & Environmental Science, 2011, 4, 2308-2315.
7. L. Kavan, J.-H. Yum, M. K. Nazeeruddin and M. Grätzel, Acs Nano, 2011, 5, 9171-9178.
8. J. Xia, L. Chen and S. Yanagida, Journal of Materials Chemistry, 2011, 21, 4644-4649.
9. J. Kwon, V. Ganapathy, Y. H. Kim, K.-D. Song, H.-G. Park, Y. Jun, P. J. Yoo and J. H. Park, Nanoscale, 2013, 5, 7838-7843.
10. M. Wang, A. M. Anghel, B. t. Marsan, N.-L. Cevey Ha, N. Pootrakulchote, S. M. Zakeeruddin and M. Grätzel, Journal of the American Chemical Society, 2009, 131, 15976-15977.
11. P. Joshi, Y. Xie, M. Ropp, D. Galipeau, S. Bailey and Q. Qiao, Energy & Environmental Science, 2009, 2, 426-429.
12. S.-H. Chang, M.-D. Lu, Y.-L. Tung and H.-Y. Tuan, ACS nano, 2013, 7, 9443-9451.
13. A. KumaráJena, Energy & Environmental Science, 2012, 5, 7001-7006.
14. G. Calogero, P. Calandra, A. Irrera, A. Sinopoli, I. Citro and G. Di Marco, Energy & Environmental Science, 2011, 4, 1838-1844.

15. H. Sun, D. Qin, S. Huang, X. Guo, D. Li, Y. Luo and Q. Meng, Energy & Environmental Science, 2011, 4, 2630-2637.
16. F. Gong, H. Wang, X. Xu, G. Zhou and Z.-S. Wang, Journal of the American Chemical Society, 2012, 134, 10953-10958.
17. J. S. Jang, D. J. Ham, E. Ramasamy, J. Lee and J. S. Lee, Chemical Communications, 2010, 46, 8600-8602.
18. Q. Jiang, G. Li, S. Liu and X. Gao, The Journal of Physical Chemistry C, 2010, 114, 13397-13401.
19. J. Burschka, V. Brault, S. Ahmad, L. Breau, M. K. Nazeeruddin, B. Marsan, S. M. Zakeeruddin and M. Grätzel, Energy & Environmental Science, 2012, 5, 6089-6097.
20. G. r. Li, F. Wang, Q. w. Jiang, X. p. Gao and P. w. Shen, Angewandte Chemie International Edition, 2010, 49, 3653-3656.
21. Y. Xiao, J. Wu, J.-Y. Lin, S.-Y. Tai and G. Yue, Journal of Materials Chemistry A, 2013, 1, 1289-1295.
22. Z. Li, F. Gong, G. Zhou and Z.-S. Wang, The Journal of Physical Chemistry C, 2013, 117, 6561-6566.
23. W. Zhou, J. Zhu, C. Cheng, J. Liu, H. Yang, C. Cong, C. Guan, X. Jia, H. J. Fan and Q. Yan, Energy & Environmental Science, 2011, 4, 4954-4961.
24. S. Yang, X. Feng, S. Ivanovici and K. Müllen, Angewandte Chemie International Edition, 2010, 49, 8408-8411.
25. Z. Dong, H. Ren, C. M. Hessel, J. Wang, R. Yu, Q. Jin, M. Yang, Z. Hu, Y. Chen and Z. Tang, Advanced Materials, 2013, 26, 905–909.
26. J. Du, J. Qi, D. Wang and Z. Tang, Energy & Environmental Science, 2012, 5, 6914-6918.
27. Y. Gu, Y. Xu and Y. Wang, ACS applied materials & interfaces, 2013, 5, 801-806.
28. W. Zhou, J. Zhu, C. Cheng, J. Liu, H. Yang, C. Cong, C. Guan, X. Jia, H. J. Fan and Q. Yan, Energy & Environmental Science, 2011, 4, 4954-4961.
29. Z. Chen, M. Zhou, Y. Cao, X. Ai, H. Yang and J. Liu, Advanced Energy Materials, 2012, 2, 95-102.
30. D. Deng, X. Pan, L. Yu, Y. Cui, Y. Jiang, J. Qi, W.-X. Li, Q. Fu, X. Ma and Q. Xue, Chemistry of Materials, 2011, 23, 1188-1193.
31. D. Wei, Y. Liu, Y. Wang, H. Zhang, L. Huang and G. Yu, Nano letters, 2009, 9, 1752-1758.
32. C. Zhang, L. Fu, N. Liu, M. Liu, Y. Wang and Z. Liu, Advanced Materials, 2011, 23, 1020-1024.
33. L. Lai, J. R. Potts, D. Zhan, L. Wang, C. K. Poh, C. Tang, H. Gong, Z. Shen, J. Lin and R. S. Ruoff, Energy & Environmental Science, 2012, 5, 7936-7942.
34. H. J. Shin, K. K. Kim, A. Benayad, S. M. Yoon, H. K. Park, I. S. Jung, M. H. Jin, H. K. Jeong, J. M. Kim and J. Y. Choi, Advanced Functional Materials, 2009, 19, 1987-1992.
35. Z. Xu, Y. Zhang, P. Li and C. Gao, ACS nano, 2012, 6, 7103-7113.
36. L. Yi, Y. Liu, N. Yang, Z. Tang, H. Zhao, G. Ma, Z. Su and D. Wang, Energy & Environmental Science, 2013, 6, 835-840.
37. G. H. Guai, M. Y. Leiw, C. M. Ng and C. M. Li, Advanced Energy Materials, 2012, 2, 334-338.
38. Q. Tai, B. Chen, F. Guo, S. Xu, H. Hu, B. Sebo and X.-Z. Zhao, Acs Nano, 2011, 5, 3795-3799.
39. Y. C. Wang, D. Y. Wang, Y. T. Jiang, H. A. Chen, C. C. Chen, K. C. Ho, H. L. Chou and C. W. Chen, Angewandte Chemie International Edition, 2013, 52, 6694-6698.
40. X. Yang, M. Yanagida and L. Han, Energy & Environmental Science, 2013, 6, 54-66.

Broader context

To solve the energy crisis and environmental pollution problems, researchers have prompted to intensively investigate solar cells which can provide clean and renewable energy to reduce the consumption of fossil fuels. Dye-sensitized solar cells (DSSCs) are promising solar cells because of their low cost and environmentally friendly characteristics. For the purpose of further cost-cutting, Platinum (Pt)-free counter electrode (CE) has been proposed to be used in the DSSCs. However, the efficiency of cells fabricated with Pt-free CEs is still lower than that of cells with Pt CEs, especially, in the cell with high efficiency of over 10%. In this work, a DSSC prepared with the novel quasi core–shell NDG/CoS catalyst as the CE showed a high short-circuit current density (20.38 mA cm^{-2}) and an energy-conversion efficiency of 10.71%, which is, as far as we know, the highest reported efficiency for a DSSC based on a Pt-free CE.